

Electronic Supplementary Material (ESI) for New Journal of Chemistry.

## Facile solvothermally method assisted g-C<sub>3</sub>N<sub>4</sub> post-grafting with aromatic amine dyes for highly photocatalytic hydrogen evolution

Xiaodi Chen,<sup>†a</sup> Hailian Bao,<sup>†a</sup> Shihang Liu,<sup>a</sup> Xingliang Liu,<sup>a</sup> Chao Zhang<sup>\*a</sup>

*a. School of Chemical Engineering, Qinghai University, Xining 810016, Qinghai, China.*

E-mail: zhangchaoqhu@126.com

### Contents

1. The TEM images of g-C <sub>3</sub> N <sub>4</sub> , g-C <sub>3</sub> N <sub>4</sub> /TPA-CNCHO, g-C <sub>3</sub> N <sub>4</sub> /PTZ-CNCHO, g-C <sub>3</sub> N <sub>4</sub> /CZ-CNCHO.	S2
2. The element map of g-C <sub>3</sub> N <sub>4</sub> /TPA-CNCHO.	S2
3. The N <sub>2</sub> adsorption desorption isotherms and pore size distribution of g-C <sub>3</sub> N <sub>4</sub> , g-C <sub>3</sub> N <sub>4</sub> /TPA-CNCHO, g-C <sub>3</sub> N <sub>4</sub> /PTZ-CNCHO and g-C <sub>3</sub> N <sub>4</sub> /CZ-CNCHO.	S3
4 The surface area and pore diameter of g-C <sub>3</sub> N <sub>4</sub> , g-C <sub>3</sub> N <sub>4</sub> /TPA-CNCHO, g-C <sub>3</sub> N <sub>4</sub> -PTZ-CNCHO and g-C <sub>3</sub> N <sub>4</sub> -CZ-CNCHO.	S3
5 XPS spectra of C1s of g-C <sub>3</sub> N <sub>4</sub> (a) and g-C <sub>3</sub> N <sub>4</sub> /PTZ-CNCHO.	S3
6 Optical photos of relevant samples.	S4
7 LSV curves of g-C <sub>3</sub> N <sub>4</sub> , g-C <sub>3</sub> N <sub>4</sub> /TPA-CNCHO, g-C <sub>3</sub> N <sub>4</sub> /PTZ-CNCHO and g-C <sub>3</sub> N <sub>4</sub> /CZ-CNCHO.	S4
8 The WCA of g-C <sub>3</sub> N <sub>4</sub> (a), g-C <sub>3</sub> N <sub>4</sub> /TPA-CNCHO (b), g-C <sub>3</sub> N <sub>4</sub> /PTZ-CNCHO (c) and g-C <sub>3</sub> N <sub>4</sub> /CZ-CNCHO (d).	S5
9 The photocatalytic hydrogen evolution rate of g-C <sub>3</sub> N <sub>4</sub> , g-C <sub>3</sub> N <sub>4</sub> /TPA-CNCHO and g-C <sub>3</sub> N <sub>4</sub> -TPA-CNCHO.	S5
10 The comparison of other dye grafted photocatalyst via Schiff's base reaction for photocatalytic H <sub>2</sub> production or other use.	S6
11 DFT calculated geometry structures and electron densities of LUMOs and HOMOs of TPA-CNCHO, PTZ-CNCHO and CZ-CNCHO at B3LYP/6-31G(d) level.	S6

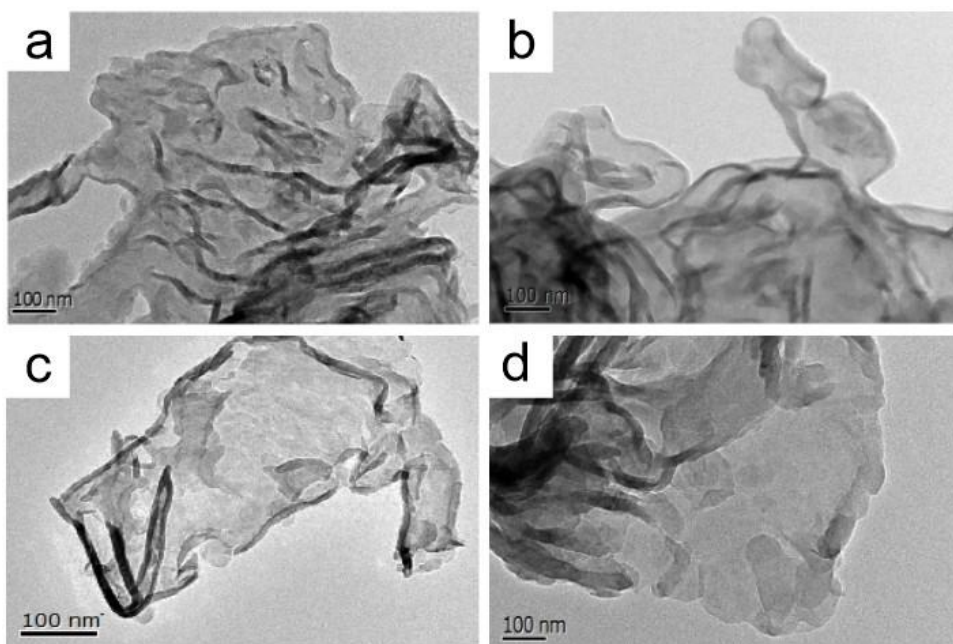


Fig. S1 The TEM images of samples (a)  $g\text{-C}_3\text{N}_4$ , (b)  $g\text{-C}_3\text{N}_4/\text{TPA-CNCHO}$ , (c)  $g\text{-C}_3\text{N}_4/\text{PTZ-CNCHO}$ , (d)  $g\text{-C}_3\text{N}_4/\text{CZ-CNCHO}$ .

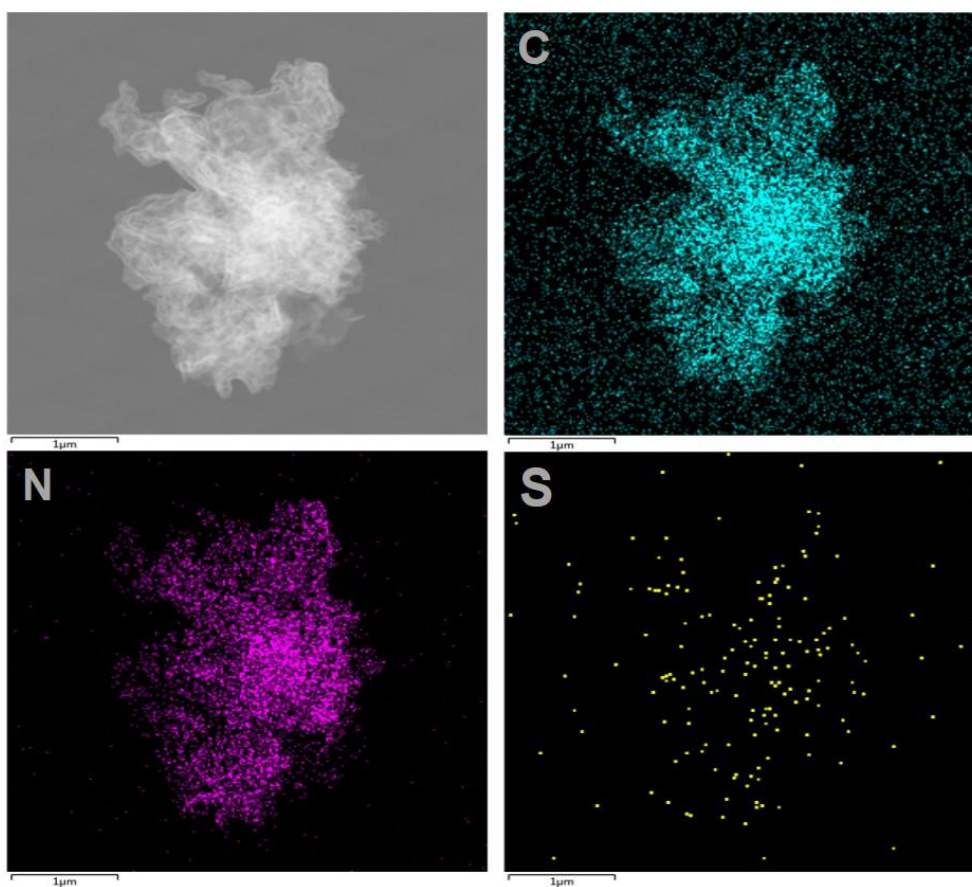


Fig. S2 The element map of  $g\text{-C}_3\text{N}_4/\text{TPA-CNCHO}$  (C (green), N (purple), S (yellow)).

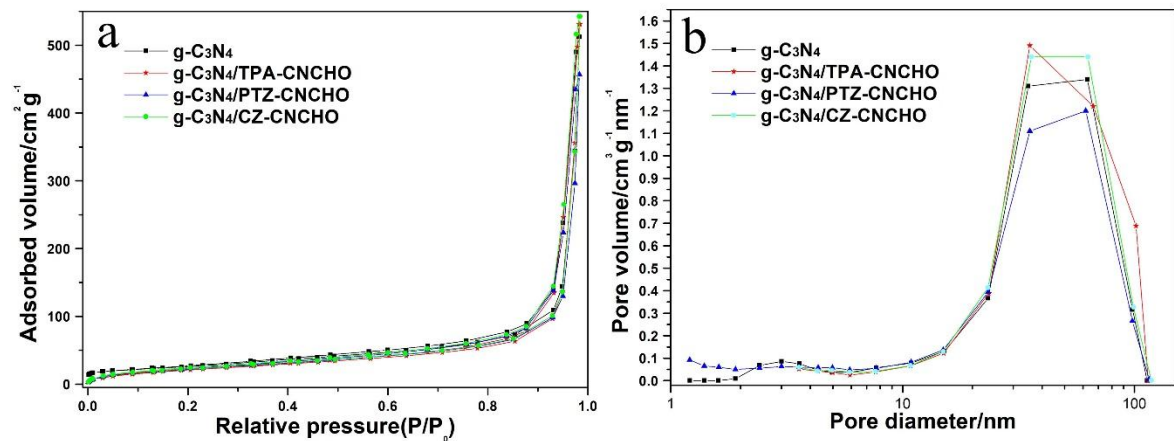


Fig. S3 The N<sub>2</sub> adsorption-desorption isotherms and pore size distribution of samples (a) g-C<sub>3</sub>N<sub>4</sub>, (b) g-C<sub>3</sub>N<sub>4</sub>/TPA-CNCHO, (c) g-C<sub>3</sub>N<sub>4</sub>/PTZ-CNCHO and (d) g-C<sub>3</sub>N<sub>4</sub>/CZ-CNCHO.

Table S1. The surface area and pore diameter of g-C<sub>3</sub>N<sub>4</sub>, g-C<sub>3</sub>N<sub>4</sub>/TPA-CNCHO, g-C<sub>3</sub>N<sub>4</sub>/PTZ-CNCHO and g-C<sub>3</sub>N<sub>4</sub>/CZ-CNCHO.

Sample	S <sub>BET</sub> (m <sup>2</sup> /g)	Pore diameter-max (nm)
g-C <sub>3</sub> N <sub>4</sub>	95.0	34.9
g-C <sub>3</sub> N <sub>4</sub> -TPA-CNCHO	82.5	35.4
g-C <sub>3</sub> N <sub>4</sub> -PTZ-CNCHO	86.6	36.1
g-C <sub>3</sub> N <sub>4</sub> -CZ-CNCHO	88.1	35.9

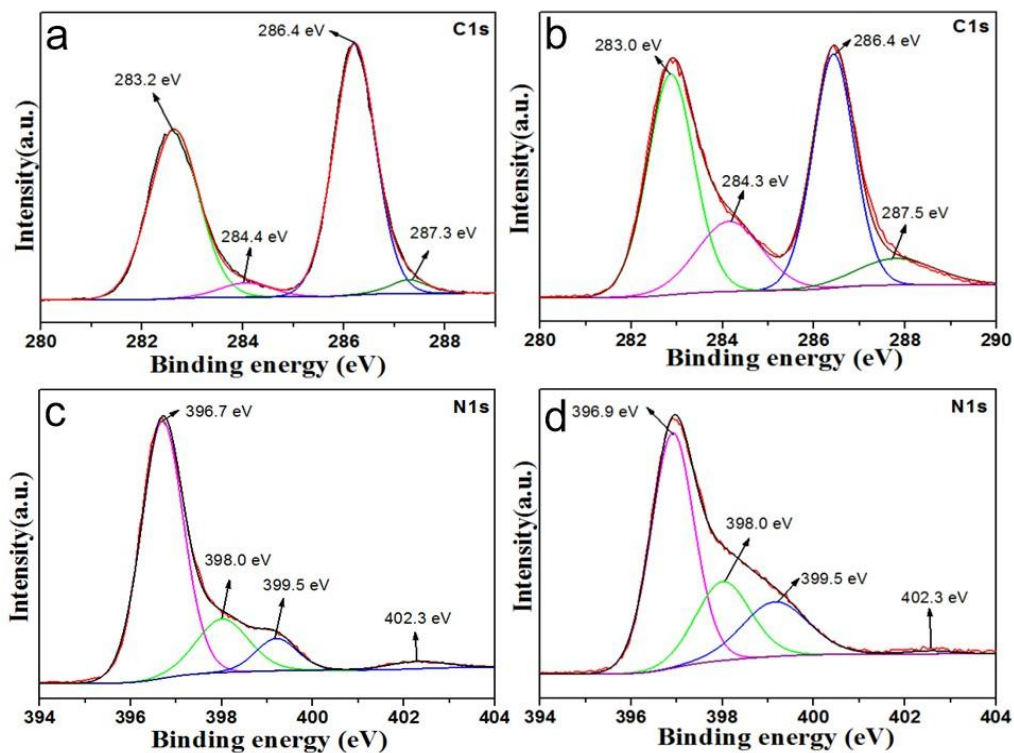


Fig. S4 XPS spectra of C1s of g-C<sub>3</sub>N<sub>4</sub> (a) and g-C<sub>3</sub>N<sub>4</sub>/PTZ-CNCHO (b), N1s of g-C<sub>3</sub>N<sub>4</sub> (c) and N1s of g-C<sub>3</sub>N<sub>4</sub>/PTZ-CNCHO (d)

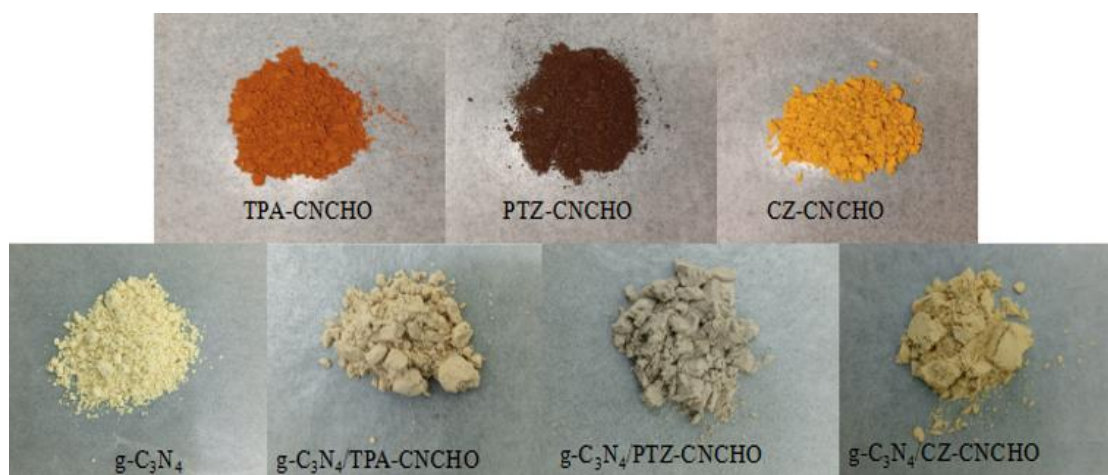


Fig. S5 Optical photos of relevant samples.

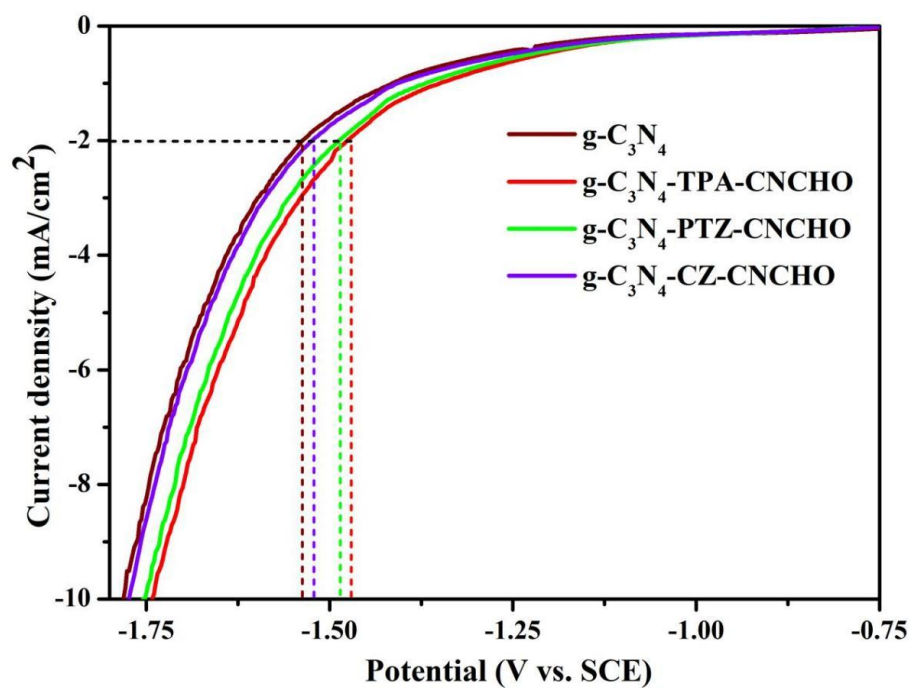


Fig. S6 LSV curves of  $g-C_3N_4$ ,  $g-C_3N_4/TPA-CNCHO$ ,  $g-C_3N_4/PTZ-CNCHO$  and  $g-C_3N_4/CZ-CNCHO$ .

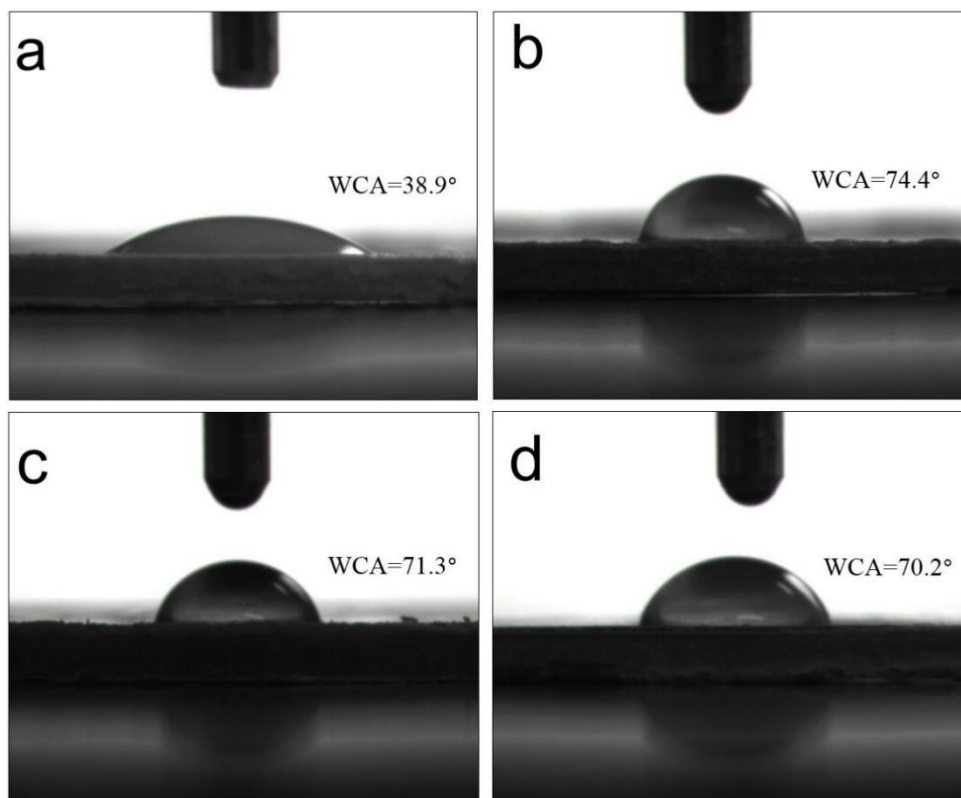


Fig. S7 The WCA of  $g\text{-C}_3\text{N}_4$  (a),  $g\text{-C}_3\text{N}_4/\text{TPA-CNCHO}$  (b),  $g\text{-C}_3\text{N}_4/\text{PTZ-CNCHO}$  (c) and  $g\text{-C}_3\text{N}_4/\text{CZ-CNCHO}$  (d).

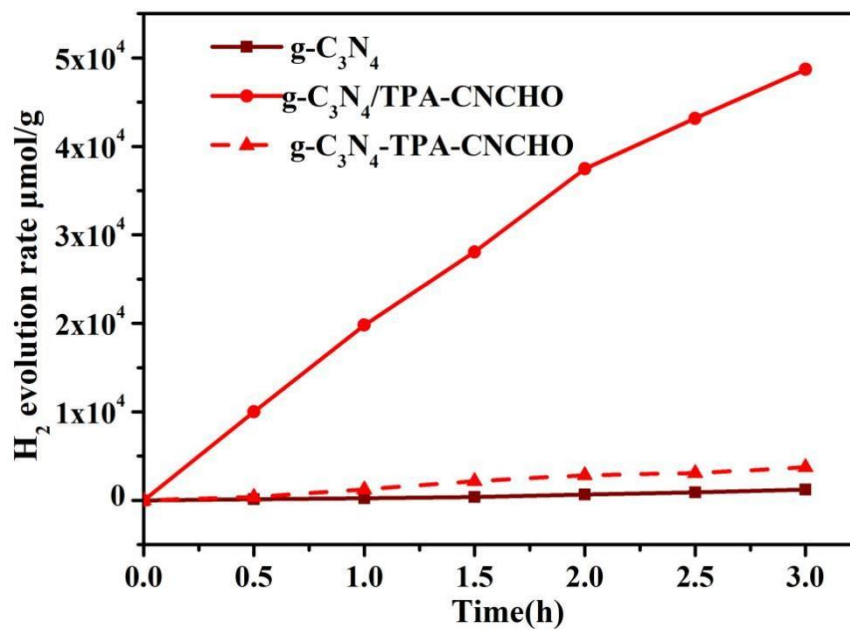


Fig. S8 The photocatalytic hydrogen evolution rate of  $g\text{-C}_3\text{N}_4$ ,  $g\text{-C}_3\text{N}_4/\text{TPA-CNCHO}$  and  $g\text{-C}_3\text{N}_4\text{-TPA-CNCHO}$ .

Table S2. The comparison of other dye grafted photocatalyst via Schiff's base reaction for photocatalytic H<sub>2</sub> production or other use.

Photocatalyst	Modification method	Modification conditions	Photocatalytic Reaction conditions	H <sub>2</sub> production activity (n times of g-C <sub>3</sub> N <sub>4</sub> )	Other photocatalytic activity	Ref.
melamine / p-benzaldehyde	copolymerization	insert gas PPL lined autoclave 250°C, 6h	triethanolamine (TEOA) $\lambda \geq 420$ nm	58.1 mmol·h <sup>-1</sup> (n=2)	none	S1
Urea/ p-benzaldehyde	Schiff's base reaction	550°C, 2h, 5°C/min	TEOA 420 nm < $\lambda$ < 780nm	226 $\mu$ mol·h <sup>-1</sup> (n=2)	none	S2
g-C <sub>3</sub> N <sub>4</sub> / p-benzaldehyde	Schiff's base reaction (solid medium)	250°C, 5h, 5°C/min	TEOA $\lambda \geq 420$ nm	92.4 $\mu$ mol·h <sup>-1</sup> (n=4.1)	none	S3
g-C <sub>3</sub> N <sub>4</sub> / Feqpy-BA	Schiff's base reaction (liquid medium)	blue LED light 24°C	TEOA $\lambda = 460$ nm	none	The number of CO <sub>2</sub> conversion is 2554 and the selectivity is 95%.	S4
TPA-CNCHO	Schiff's base reaction	insert gas, DDM	AA $\lambda \geq 400$ nm	16232.7 $\mu$ mol·h <sup>-1</sup> ·g <sup>-1</sup> (n=40) 13266.9 $\mu$ mol·h <sup>-1</sup> ·g <sup>-1</sup> (n=33)	none	this work
PTZ-CNCHO	Schiff's base reaction (liquid medium)	240°C, 15h		11822.8 $\mu$ mol·h <sup>-1</sup> ·g <sup>-1</sup> (n=29)		
CZ-CNCHO						

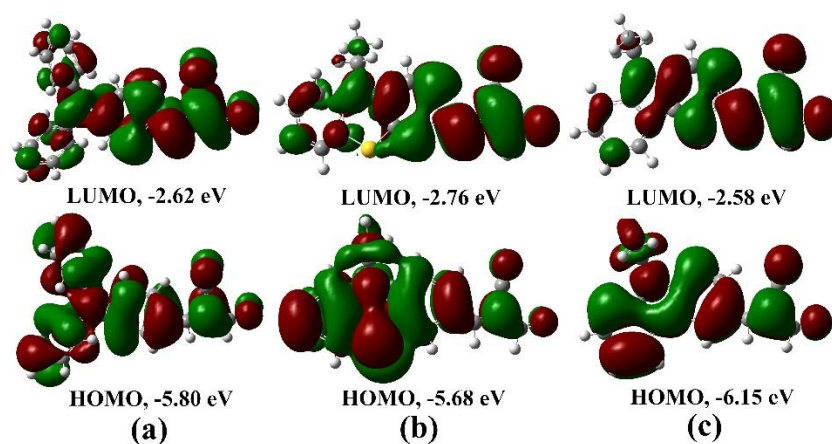


Fig. S9 DFT calculated geometry structures and electron densities of LUMOs and HOMOs of (a) TPA-CNCHO, (b) PTZ-CNCHO and (c) CZ-CNCHO at B3LYP/6-31G(d) level.

## References

S1 X. Huang, Z. Wu, H. Zheng, W. Dong, G. Wang, A sustainable method toward melamine-based conjugated polymer semiconductors for efficient photocatalytic hydrogen production under visible light, *Green Chem.*, 2017,

20, 664-670.

S2 X. Fan, L. Zhang, M. Wang, W. Huang, Y. Zhou, M. Li, R. Cheng, J. Shi, Constructing carbon-nitride-based copolymers via Schiff base chemistry for visible-light photocatalytic hydrogen evolution, *Appl. Catal. B Environ.*, 2015, 182, 68-73.

S3 J. Tian, L. Zhang, X. Fan, Y. Zhou, M. Wang, R. Cheng, M. Li, X. Kan, X. Jin, Z. Liu, Y. Gao, J. Shi, A post-grafting strategy to modify g-C<sub>3</sub>N<sub>4</sub> with aromatic heterocycles for enhanced photocatalytic activity, *J. Mater. Chem. A*, 2016, 4, 13814-13821.

S4 Y. Wei, L. Chen, H. Chen, L. Cai, G. Tan, Y. Qiu, Q. Xiang, G. Chen, T. Lau, M. Robert, Highly efficient photocatalytic reduction of CO<sub>2</sub> to CO by in situ formation of a hybrid catalytic system based on molecular iron quaterpyridine covalently linked to carbon nitride, *Angew. Chem., Int. Ed.*, 2022. 10.1002 /ange202116832.